Cone Penetration Testing 2022 – Gottardi & Tonni (eds)

Application of two novel CPTu-based stratification models

M.S. Farhadi & T. Länsivaara
Faculty of Built Environment, Department of Civil Engineering, TERRA Research Center
Tampere University, Tampere, Finland

J.-S. L'Heureux & T. Lunne
Norwegian Geotechnical Institute, Geotechnics and Natural Hazards, Oslo, Norway

ABSTRACT: Two novel CPTu-based stratification models are applied to the measurements at four Norwegian sites, including a broad range of soil behavior types (SBTs). The two models, called RIGTOSS and SIGTOSS, are developed based on the recently proposed integrated Game Theory-optimization subground stratification (-IGTOSS) model. The RIGTOSS model includes two submodels classifying the SBTs based on either the F_r-Q_t or B_q-Q_t charts by Robertson (1990); and similarly, the SIGTOSS model includes two submodels classifying the SBTs based on either the F_r-Q_t or $(\Delta u_2/\sigma' v_0)$ Q_t charts by Schneider et al. (2012). The resulting stratification profiles of the four submodels were compared with the ones provided by experts, derived from extensive field and experimental testing. Similarity was observed and the results are promising. Differences at this stage can be attributed to incompatibility of the classification charts with the Norwegian soils and more specifically soil heterogeneities at the Øysand test site.

1 INTRODUCTION

A significant advantage of cone penetration test is the continuity of measurements in depth. This valuable feature can contribute to a better understanding of subground, which may not be obtained only from sampling. As an example, it can lead to one of the main applications of CPTu testing, which is the stratification and classification of the soil behaviour type (SBT). Currently, the stratification-classification needs combining CPTu measurements with experimental and probably other field tests. However, it is desirable to stratify and classify soils only based on the CPTu measurements, which is targeted in this study.

The CPTu-based stratification-classification has been extensively investigated. Initially, a generally applicable method was sought to classify soils based on the CPTu measurements, which resulted into several classification charts (Robertson 1990, Schneider et al. 2012, Eslami et al. 2017). Despite the breakthroughs, the observed inaccuracies of the charts for different sites have left the question open, and researchers are still proposing soil-type- or site-specific classification charts (Ricceri et al. 2002, Gylland et al. 2017). However, using only the classification charts could not provide accurate stratification profiles while they represented largely high number of strata especially in highly variable soils. Therefore, several researchers focused on combining classification charts with computational methods for stratifying soils based on CPTu measurements (Ching et al. 2015, Wang et al. 2019, Shuku et al. 2020).

In Tampere university, Tampere, Finland, a novel CPT-based stratification-classification model, named -IGTOSS here, is proposed integrating several computational models: a Game Theory model, the evolutionary Grey Wolf Optimizer (GWO) and the classification chart proposed by Robertson in 1990 (Farhadi & Länsivaara 2021). It was previously evaluated based on several CPTu tests in Taiwan and the US. In this study, the model is developed further including three other SBT classification charts. Then, it is applied to several CPTu tests from Norway containing a broad range of SBTs.

2 -IGTOSS MODEL

2.1 *Normalized CPTu parameters*

The utilized normalized parameters interpreted from the CPTu measurements are (Schneider et al. 2012):

i) Normalized cone tip resistance, Q_t:

$$Q_t = \frac{q_n}{\sigma'_{v0}} = \frac{q_t - \sigma_{v0}}{\sigma'_{v0}} \quad (1)$$

DOI: 10.1201/9781003308829-55

ii) Friction ratio, F_r:

$$F_r = \frac{f_s}{q_n} \times 100 = \frac{f_s}{q_t - \sigma_{v0}} \times 100 \qquad (2)$$

iii) Pore pressure ratio, B_q:

$$B_q = \frac{\Delta u_2}{q_n} = \frac{u_2 - u_0}{q_t - \sigma_{v0}} \qquad (3)$$

iv) Normalized excess pore pressure, $\Delta u_2/\sigma'_{v0}$, which equals $B_q Q_t$;

where, q_n is the net corrected cone tip resistance, σ'_{v0} is the effective vertical stress, σ_{v0} is the total vertical stress, q_t is the total corrected cone tip resistance, f_s is sleeve friction, u_2 is the pore pressure measured at the cone shoulder, u_0 is the in-situ pore pressure prior to cone penetration, and Δu_2 is the excess pore pressure measured at the cone shoulder in penetration. As generally utilized, q_t is the measured cone tip resistance, q_c, corrected based on water content and unequal end effect of the piezometer: $q_t = q_c + u_2(1-a)$, where, a is the cone area ratio.

2.2 *Developed stratification model*

The basics of the stratification model are described in Farhadi & Länsivaara (2021). In this study, it has been developed further containing three other classification charts. A concise flowchart of the modified model is presented in Figure 1.

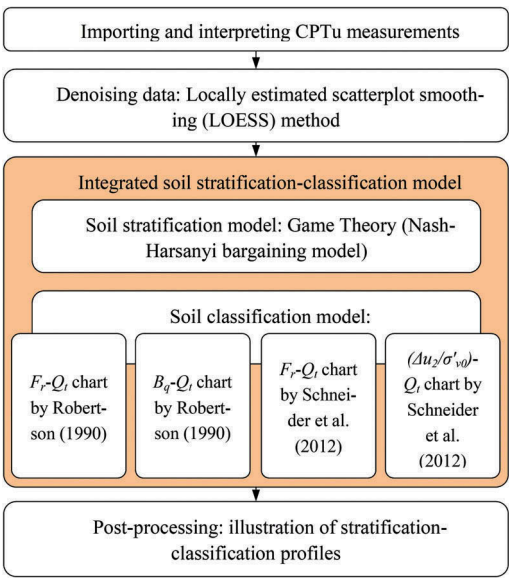

Figure 1. Concise flowchart of the proposed (R/S)ITGOSS model(s).

As illustrated in Figure 1, in the *first step*, the CPTu data are imported and interpreted. A constant soil unit weight, γ, for the whole depth of cone penetration is used to interpret Q_t, F_r, B_q and $\Delta u_2/\sigma'_{v0}$.

In the *second step*, the interpreted data is smoothed using a spatial regression method, called locally estimated scatterplot smoothing (LOESS). 1% of data is used as the spatial regression range.

In the *third step*, the integrated stratification-classification model specifies the strata boundaries depths, using a Game Theory model, as described in Farhadi & Länsivaara (2021). Then, the SBT is determined from a classification chart, in each of the following submodels:

a) RIGTOSS$_{Fr\text{-}Qt}$ based on the F_r-Q_t chart by Robertson (1990),
b) RIGTOSS$_{Bq\text{-}Qt}$ based on the B_q-Q_t chart by Robertson (1990),
c) SIGTOSS$_{Fr\text{-}Qt}$ based on the F_r-Q_t chart by Schneider et al. (2012),
d) SIGTOSS$_{(\Delta u_2/\sigma'_{v0})}$ – Q$_t$ based on the $(\Delta u_2/\sigma'_{v0})$–$Q_t$ chart by Schneider et al. (2012).

The introductory R or S letters in the names of the RIGTOSS and SIGTOSS models indicate the utilized classification charts.

In the charts by Robertson (1990), the SBTs are defined as:

1. *Sensitive, fine-grained*
2. *Organic soils - peats*
3. *Clays - clay to silty clay*
4. *Silt mixtures - clayey silt to silty clay*
5. *Sand mixtures-silty sand to sandy silt*
6. *Sands, clean sand to silty sand*
7. *Gravelly sand to sand*
8. *Very stiff sand to clayey (heavily overconsolidated or cemented) sand*
9. *Very stiff fine-grained*

In the charts by Schneider et al. (2012), the SBTs are defined as:

1a. Low-I_R clays (I_R=G/S_u; where, I_R, G and S_u represent rigidity index, shear modulus, and undrained strength, respectively)
1b. Clays
1c. Sensitive clays
3. Silts and transitional soils
2. Essentially drained sands and sand mixtures

In the *final step*, the identified SBTs of the strata are plotted three-dimensionally with colored contours, as explained in Farhadi & Länsivaara (2021).

The interested readers may contact the first author for the MATLAB code; which will be probably described further in a separate paper in future.

3 TEST SITES

The developed (R/S)IGTOSS models are applied to the CPTu data from four sites in Norway (Figure 2):

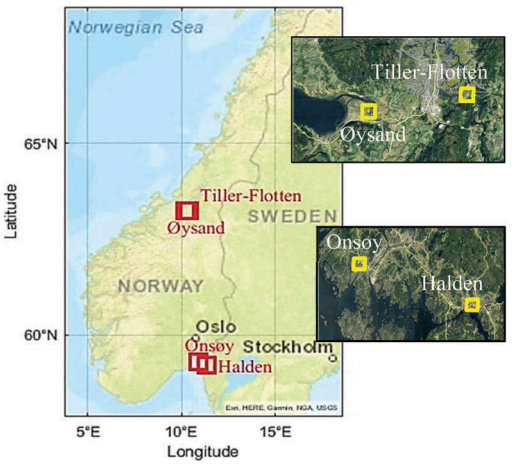

Figure 2. Location of the test sites in Norway (provided by MATLAB, hosted by Esri, and Google Earth Pro).

Table 1. Soil properties of the test sites, in brief (Blaker et al. 2019, Gundersen et al. 2019, Quinteros et al. 2019, and L'Heureux et al. 2019).

	Halden		Onsøy		Øysand		T-F*	
Property	min	max	min	max	min	max	min	max
w_n** (%)	20	35	45	65	12	33	30	53
γ(kN/m^3)	18.3	20.8	15	19	13	23	16.8	19.1
FC (%)	15	99						
CC (%)	2	17	45	68	0	18	40	70
LL (%)	27.5	37.5	46	77			27	53
I_p (%)	6	13	25	50			7	29
S_t			5	19			0	360
OC (%)			30	50				
SC (g/L)			8	36			2	3

* T-F stands for Tiller-Flotten.

** w_n: natural water content; γ: unit weight; *FC*: fines content; *CC*: clay content; *LL*: liquid limit; I_p: plasticity index; S_t: sensitivity; *OC*: organic content; and *SC*: salt content.

a silt site at Halden, a soft clay site at Onsøy, a medium dense sand site at Øysand, and a quick clay site at Tiller-Flotten (L'Heureux & Lunne 2019).

The Halden site consists of a natural fjord marine deposit including mostly a low plasticity silt. A majority of bulky angular grains was observed at the scanning electron microscope (SEM) test: 41% quartz and 42% feldspar (Carroll & Paniagua 2018). Water table was 2.5 m below the surface. Further soil properties for all sites are presented in summary in Table 1.

The Onsøy site consists of a marine clay deposit with similar behaviour as that observed in Canada, Japan, Southeast Asia, Sweden, and Finland. The site has a thick layer of uniform very soft to soft clay.

The Øysand site consists of a 20 m thick glaciofluvial mostly sandy deposit. The site includes several strata of gravelly sand (fluvial deposit), fine silty sand (deltaic soils), and clay-and-silt. The sand layer includes fine to medium uniform sand, predominantly of quartz minerals, some plagioclase and micas.

The Tiller-Flotten site consists of marine and glaciomarine sediments with a thick layer of sensitive clay from 8 m below terrain.

4 RESULTS AND DISCUSSION

4.1 *Denoising data*

Figure 3 shows the interpreted smoothed F_r, Q_t, B_q and $\Delta u_2/\sigma'_{v0}$ parameters for tests HALC19 and HALC20. It can be observed that the major variations are preserved after smoothing, and the minor sharp variations are smoothly approximated. Thus, the smoothing rarely impacts the resulting stratification profile while the model finds the strata boundaries

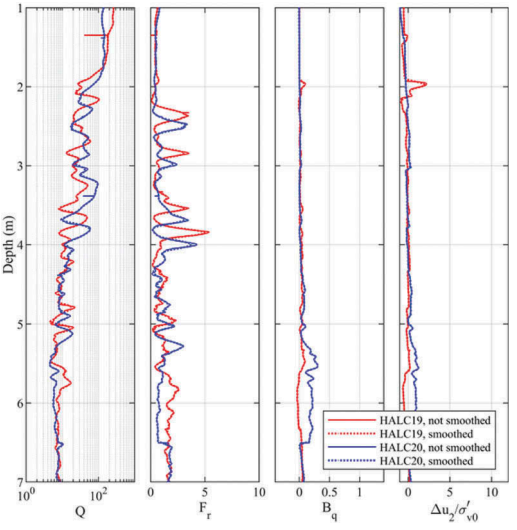

Figure 3. Illustration of the smoothing impact on the parameters interpreted from the CPTu tests at the Halden site.

mostly based on the large change points. However, most importantly it removes the outliers in data, such as those caused by stopping the cone penetration.

4.2 *Stratification-classification profiles*

4.2.1 *Halden*

Figure 4 illustrates the stratification-classification profiles for test HALC19.

Figures 4a-4d show that the interpreted parameters look similar before and after smoothing; although, several abrupt changes are removed. For

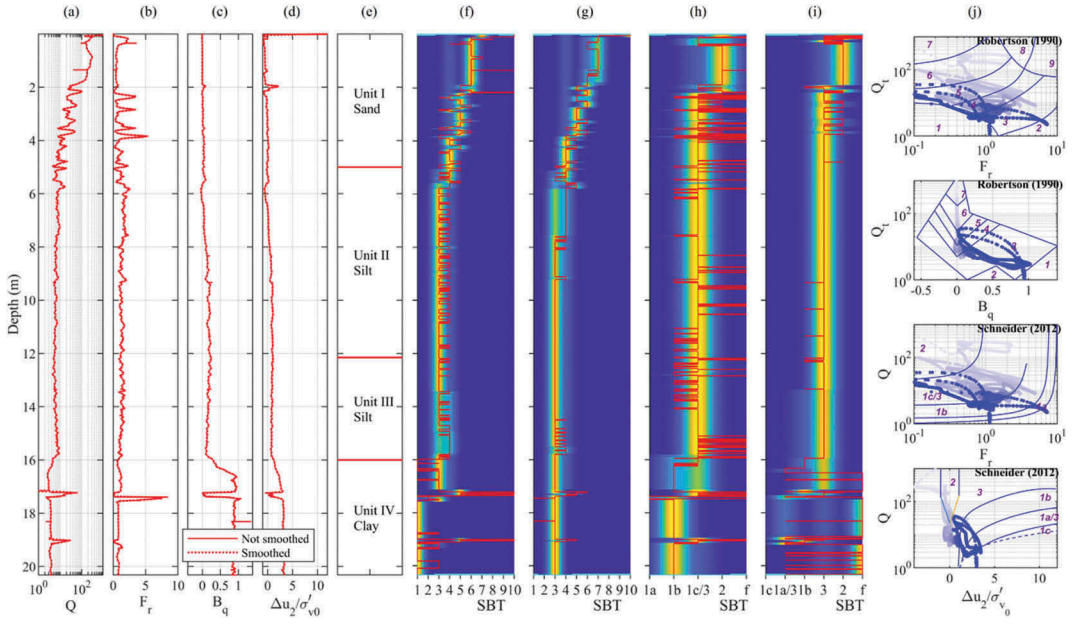

Figure 4. Illustration of CPTu measurements, experts stratification profile, RIGTOSS and SIGTOSS stratification profiles, and distribution of CPTu measurements on classification charts, for test HALC19, from Halden investigation site: a-d) smoothed versus unsmoothed interpreted CPTu parameters, e) expert-based stratification reported for Halden site (Blaker et al. 2019), f-i) directly chart-based stratification profile, presented by a solid line, versus the profiles provided by the RIGTOSS$_{Fr\text{-}Qt}$, RIGTOSS$_{Bq\text{-}Qt}$, SIGTOSS$_{Fr\text{-}Qt}$ and SIGTOSS$_{(\Delta u2/\sigma' v0)-Qt}$ models, respectively, and, j) distribution of measurements points on the classification charts (the color of data points gets darker with depth). In (R/S)IGTOSS stratification profiles, SBTs of '10′ and 'f' mean that the data points located out of the boundaries of the classification charts. [In profiles, the yellow color shows higher probability of the SBT.].

example, in Figure 4a, two sudden changes at approximate depths of 0.5 and 1.4 m are removed after smoothing.

Figure 4e illustrates the experts' judgement based on the in-situ and laboratory tests performed by Norwegian Geotechnical Institute (NGI). Four main soil deposits are identified: a loose to medium dense silty clayey sand from 0 to 5 m (Unit I), two clayey silt layers with the same geologic origin and almost the same material (Units II and III), and a deeper unit consisting of medium stiff clay (Unit IV) (Blaker et al. 2019).

In Figures 4f-4i, the solid lines show the stratification profiles after using directly the classification charts. A large number of thin layers can be identified with dissimilar SBTs, compared with the (R/S) IGTOSS contoured profiles (Figures 4f-4i) and the experts' profile (Figure 4e). The identification of numerous strata originates from the location of the CPTu measurements points on a classification chart; which may be located close to the SBT boundary lines, but on different sides.

The colour-contoured profiles in Figures 4h-4i show that the SIGTOSS$_{Fr\text{-}Qt}$ and SIGTOSS-$_{(\Delta u_2/\sigma'_{v0})-Q_t}$ models indicate three thick strata. However, the RIGTOSS$_{Fr\text{-}Qt}$ and RIGTOSS$_{Bq\text{-}Qt}$ models indicate approximately 5 thick strata (Figures 4f-4g). Thinner layers can be observed with different probabilities at these thick strata.

Figure 4j illustrates the location of the CPTu measurements on the classification charts. The colour of the points gets darker with depth. They show the variability of the soil at the Halden site. In addition, comparing them with Figures 4f-4i showed that the (R/S)IGTOSS profiles are correctly determined.

4.2.2 *Onsøy*

Figure 5 shows the (R/S)IGTOSS results for tests ONSC19, ONSC20, and ONSC21, performed at the south-east corner of the Onsøy site. The distances between their locations were less than 2.1 m.

Figures 5a-5d indicate the impact of the smoothing method, and an appropriate repeatability of CPTu tests; although, the ONSC20 measurements deviate from the other two tests at some depths.

Comparing Figures 5e with two sets of Figures 5f-5i and 5j-5m indicates a generally appropriate similarity in recognizing the soil type as clay; although, the strata identified by experts are more than the strata identified by the (R/S)IGTOSS models. On the other hand, several thin layers are identified by the (R/S)IGTOSS models.

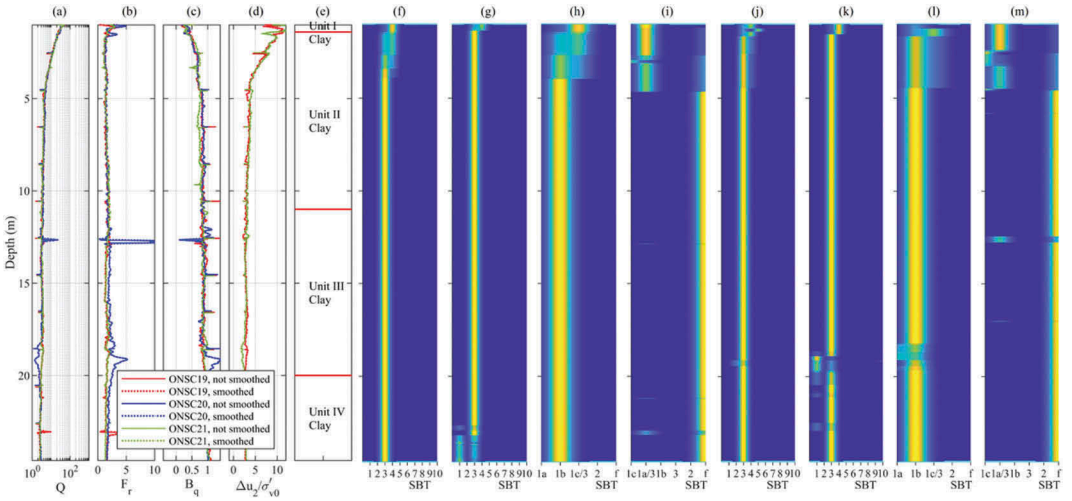

Figure 5. Comparison of the CPTu measurements at the Onsøy test site: a-e) smoothed and unsmoothed measurements of tests ONSC19, ONSC20, and ONSC21, f-i) respectively, RIGTOSS$_{Fr\text{-}Qt}$, RIGTOSS$_{Bq\text{-}Qt}$, SIGTOSS$_{Fr\text{-}Qt}$ and SIGTOSS$_{(\Delta u2/\sigma' v0)\text{-}Qt}$ profiles for ONSC19, and, j-m) respectively, RIGTOSS$_{Fr\text{-}Qt}$, RIGTOSS$_{Bq\text{-}Qt}$, SIGTOSS$_{Fr\text{-}Qt}$ and SIGTOSS$_{(\Delta u2/\sigma' v0)\text{-}Qt}$ profiles for test ONSC20.

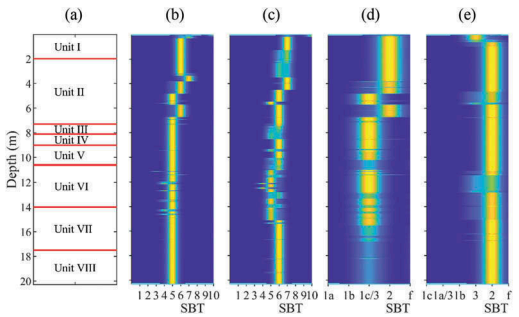

Figure 6. Comparison of (a) experts' stratification profile with the (b) RIGTOSS$_{Fr\text{-}Qt}$, (c) RIGTOSS$_{Bq\text{-}Qt}$, (d) SIGTOSS$_{Fr\text{-}Qt}$, and (e) SIGTOSS$_{(\Delta u2/\sigma' v0)-Qt}$ models profiles, for test OYSC40, Øysand site. In the experts' profile, Unit I is sand (silty, fine; layers and seams of medium to coarse sand), Unit II is sand (fine to coarse, gravelly), Unit III is sand (fine, traces of organic material), Unit IV is sand (fine to medium, silty), Unit V is sand (medium to coarse, gravelly), Unit VI is sand (fine to medium, silty), Unit VII is silt (sandy, clayey), and Unit VIII is sand (fine to medium, silty) (Quinteros et al. 2019).

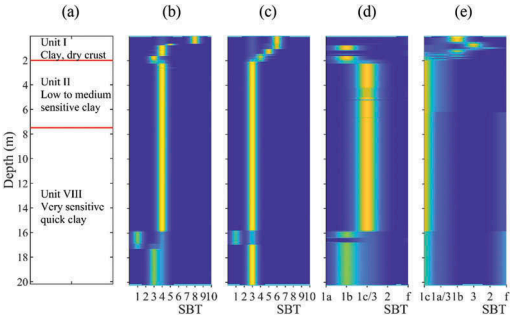

Figure 7. Comparison of (a) experts' stratification profile with the (b) RIGTOSS$_{Fr\text{-}Qt}$, (c) RIGTOSS$_{Bq\text{-}Qt}$, (d) SIGTOSS$_{Fr\text{-}Qt}$, and (e) SIGTOSS$_{(\Delta u2/\sigma' v0)-Qt}$ models profiles, for test TILC17, Tiller-Flotten site (L'Heureux et al. 2019).

4.2.3 *Øysand*

Figure 6 shows the experts' stratification profile (Quinteros et al. 2019) compared with the (R/S)IGTOSS profiles for test OYSC40. The experts recognized several strata of sandy soils for the whole depth, except for Unit VII, which is mainly silty. Similarly, the (R/S) IGTOSS models identified mostly sand mixtures; except SIGTOSS$_{Fr\text{-}Qt}$ that identified silts and transitional soils, i.e. SBT=3, but at depths different from Unit VII. In general, the strata boundaries recognized by the models differ significantly from the experts' judgement at Øysand; although, the SBT characterization is quite similar.

4.2.4 *Tiller-Flotten*

Figure 7 compares the SBT profiles by the experts (L'Heureux et al. 2019) and (R/S)IGTOSS models for test TILC17. It is interesting that only the SIGTOSS$_{(\Delta u2/\sigma' v0)-Qt}$ model has clearly recognized the sensitive clays. Albeit, in the SIGTOSS$_{Fr\text{-}Qt}$ model the SBT has been mainly either 1c, sensitive clay, or 3, i.e. silts and transitional soils. Besides, the RIGTOSS model could not recognize the sensitive clays, i.e. SBT = 1, well; however, it found them as clays or silt mixtures. Further, it can be observed that the strata change depths are recognized differently by the models and the experts.

4.2.5 *Comparison of classification charts*

Comparing the $RIGTOSS_{Fr\text{-}Qt}$ and $RIGTOSS_{Bq\text{-}Qt}$ profiles in Figures 4-7 for each test, indicates almost similar stratification profiles. However, differences can be due to the different numbers of SBT zones on the classification charts, and different interpreted parameters used in each of them.

Similarly, comparing the $SIGTOSS_{Fr\text{-}Qt}$ and $SIGTOSS_{(\Delta u2/\sigma' v0)-Qt}$ profiles in Figures 4-7 indicates almost similar profiles with respect to the strata boundaries depths; but the SBT differences are visible. Besides, data points may be located out of the boundaries of the $SIGTOSS_{(\Delta u2/\sigma' v0)-Qt}$ chart, i.e. SBT='f' in the profiles. This may originate from several factors, such as the incompatibility of the chart with the Norwegian soils, using different interpretation methods in this study in contrast to the ones used in Schneider et al. (2012), and the small zone of '1c' on the chart.

Figures 4-7 indicated that judging based on the Schneider's chart might have advantage over using the Robertson chart for the Norwegian fine-grained soils; although, it can be confusing to differentiate clays from silts based on the Schneider's chart.

On the other hand, comparing the RIGTOSS and SIGTOSS profiles, less strata are determined based on the charts proposed by Schneider et al. (2012), while they include less SBT zones. Then, it may affect the precision of stratification and the recognized number of strata; which can be observed in Figures 5 and 6, as examples.

5 CONCLUSIONS

A stratification-classification model by Farhadi & Länsivaara (2021) is developed further in this study to include different CPTu-based soil classification charts. The developed models are applied to four Norwegian soils. As observed, the stratification profiles of the models are comparable with the profiles presented by experts –which resulted from extensive field and laboratory experiments. However, there are still differences between them, principally originating from:

- using different soil classification viewpoints or parameters implemented in the available classification charts,
- incompatibility of the used classification charts with the Norwegian soils, especially for fine-grained soils, and,
- spatial variability of soils, resulting into almost different stratification profiles for the CPTu tests performed close to each other.

In addition, it was observed that the CPTu measurements points may be located out of the bounds of the Schneider's $\Delta u_2/\sigma'_{v0} - Q$ chart, which could be caused by the incompatibility of the chart with the Norwegian soils.

ACKNOWLEDGEMENT

The authors acknowledge the support from Norwegian GeoTest Sites infrastructure (NGTS) for access to data. The study was also supported partly by Tekniikan Edistämissäätiö (Finnish Foundation for Technology Promotion), Grant No. JNR. 8375, for the first author.

REFERENCES

Blaker, Ø., Carroll, R., Paniagua Lopez, A.P., Degroot, D. J. & L'Heureux, J.-S. 2019. Halden research site: geotechnical characterization of a post glacial silt. *AIMS Geosciences* 5(2): 184–234. doi: 10.3934/geosci.2019.2.184.

Carroll, R. & Paniagua, P. 2018. Variable rate of penetration and dissipation test results in a natural silty soil. *Cone Penetration Testing 2018*. CRC Press.

Ching, J., Wang, J.-S., Juang, C.H. & Ku, C.-S. 2015. Cone penetration test (CPT)-based stratigraphic profiling using the wavelet transform modulus maxima method. *Canadian Geotechnical Journal* 52(12): 1993–2007. https://doi.org/10.1139/cgj-2015-0027.

Eslami, A., Alimirzaei, M., Aflaki, E. & Molaabasi, H. 2017. Deltaic soil behavior classification using CPTu records—Proposed approach and applied to fifty-four case histories. *Marine Georesources & Geotechnology* 35: 62–79. doi: 10.1080/1064119X.2015.1102185.

Farhadi, M.S. & Länsivaara, T. 2021. Development of an integrated game theory-optimization subground stratification model using cone penetration test (CPT) measurements. *Engineering with Computers*. https://doi.org/10.1007/s00366-020-01243-0.

Gundersen, A., Hansen, R., Lunne, T., L'Heureux, J.-S. & Strandvik, S.O. 2019. Characterization and engineering properties of the NGTS Onsøy soft clay site. *AIMS Geosciences* 5: 665–703. doi: 10.3934/geosci.2019.3.665.

Gylland, A.S., Sandven, R., Montafia, A., Pfaffhuber, A.A., Kåsin, K. & Long, M. 2017. CPTU classification diagrams for identification of sensitive clays. *Landslides in Sensitive Clays*. Springer.

L'Heureux, J.-S., Lindgård, A. & Emdal, A. 2019. The Tiller–Flotten research site: Geotechnical characterization of a very sensitive clay deposit. *AIMS Geosciences* 5(4): 831–867. doi: 10.3934/geosci.2019.4.831.

L'heureux, J.-S. & Lunne, T. 2020. Characterization and engineering properties of natural soils used for geotesting. *AIMS Geosciences* 6(1): 35–53. doi: 10.3934/geosci.2020004.

L'Heureux, J.-S., Carroll, R., Lacasse, S., Lunne, T., Strandvik, S.O., Degago, S., Instanes, A., Nordal, S. & Sinitsyn, A. 2017. New Research Benchmark Test Sites in Norway. *Geotechnical Frontiers 2017*.

Quinteros, S., Gundersen, A., L'Heureux, J.-S., Carraro, A.H. & Jardine, R. 2019. Øysand research site: Geotechnical characterisation of deltaic sandy-silty soils. *AIMS Geosciences* 5(4): 750–783. doi: 10.3934/geosci.2019.4.750

Ricceri, G., Simonini, P. & Cola, S. 2002. Applicability of piezocone and dilatometer to characterize the soils of the Venice Lagoon. *Geotechnical & Geological Engineering* 20: 89–121. doi: 10.1023/A:1015043911091.

Robertson, P.K. 1990. Soil classification using the cone penetration test. *Canadian Geotechnical Journal* 27(1): 151–158. https://doi.org/10.1139/t90-014.

Schneider, J.A., Hotstream, J.N., Mayne, P.W. & Randolph, M. F. 2012. Comparing CPTU Q–F and Q–$\Delta u_2/\sigma_{v0}'$ soil classification charts. *Géotechnique Letters* 2(4): 209–215. https://doi.org/10.1680/geolett.12.00044.

Shuku, T., Phoon, K.-K. & Yoshida, I. 2020. Trend estimation and layer boundary detection in depth-dependent soil data using sparse Bayesianlasso. *Computers and Geotechnics* 128, 103845. https://doi.org/10.1016/j.compgeo.2020.103845.

Wang, H., Wang, X., Wellmann, J.F. & Liang, R.Y. 2019. A Bayesian unsupervised learning approach for identifying soil stratification using cone penetration data. *Canadian Geotechnical Journal* 56(8): 1184–1205. doi: 10.1139/cgj-2017-0709.